Development 136, 2081-2089 (2009) doi:10.1242/dev.033548

Expression of the *Arf* tumor suppressor gene is controlled by Tgfβ2 during development

Natalie E. Freeman-Anderson[1,*], Yanbin Zheng[2,*], Amy C. McCalla-Martin[1], Louise M. Treanor[1], Yi D. Zhao[2], Phillip M. Garfin[2], Tong-Chuan He[3], Michelle N. Mary[1], J. Derek Thornton[1], Colleen Anderson[1], Melissa Gibbons[2], Raya Saab[4], Shannon H. Baumer[2], John M. Cunningham[2] and Stephen X. Skapek[2,†]

The *Arf* tumor suppressor (also known as *Cdkn2a*) acts as an oncogene sensor induced by 'abnormal' mitogenic signals in incipient cancer cells. It also plays a crucial role in embryonic development: newborn mice lacking *Arf* are blind due to a pathological process resembling severe persistent hyperplastic primary vitreous (PHPV), a human eye disease. The cell-intrinsic mechanism implied in the oncogene sensor model seems unlikely to explain *Arf* regulation during embryo development. Instead, transforming growth factor β2 (Tgfβ2) might control *Arf* expression, as we show that mice lacking Tgfβ2 have primary vitreous hyperplasia similar to $Arf^{-/-}$ mice. Consistent with a potential linear pathway, Tgfβ2 induces *Arf* transcription and $p19^{Arf}$ expression in cultured mouse embryo fibroblasts (MEFs); and Tgfβ2-dependent cell cycle arrest in MEFs is maintained in an *Arf*-dependent manner. Using a new model in which *Arf* expression can be tracked by β-galactosidase activity in $Arf^{lacZ/+}$ mice, we show that Tgfβ2 is required for *Arf* transcription in the developing vitreous as well as in the cornea and the umbilical arteries, two previously unrecognized sites of *Arf* expression. Chemical and genetic strategies show that *Arf* promoter induction depends on Tgfβ receptor activation of Smad proteins; the induction correlates with Smad2 phosphorylation in MEFs and *Arf*-expressing cells in vivo. Chromatin immunoprecipitation shows that Smads bind to genomic DNA proximal to *Arf* exon 1β. In summary, Tgfβ2 and $p19^{Arf}$ act in a linear pathway during embryonic development. We present the first evidence that $p19^{Arf}$ expression can be coupled to extracellular cues in normal cells and suggest a new mechanism for *Arf* control in tumor cells.

KEY WORDS: Arf tumor suppressor gene, Ocular development, Tgf beta, Mouse

INTRODUCTION

It is now well recognized that $p19^{Arf}$, encoded by *Arf* (*Cdkn2a* – Mouse Genome Informatics) at the mammalian *Arf/Ink4a* locus (Kamijo et al., 1997), has a range of *p53*-dependent and -independent effects that contribute to its anti-cancer activity (Sherr, 2006). However, how the expression of $p19^{Arf}$ is regulated is much less well understood. It was first discovered to be induced in cultured mouse embryo fibroblasts (MEFs) by what has been termed 'culture shock' (Kamijo et al., 1997; Sherr and DePinho, 2000) and by the expression of certain oncogenes (de Stanchina et al., 1998; Palmero et al., 1999; Zindy et al., 1998). Implicit in the 'oncogene sensor' model for $p19^{Arf}$ is that *Arf* expression is controlled by cell-intrinsic mechanisms. However, this concept has not been rigorously tested. We recently discovered that *Arf* is also expressed in a subset of perivascular cells enveloping the hyaloid vasculature in the vitreous of the developing eye (Martin et al., 2004; McKeller et al., 2002). The hyaloid vessels are unusual because they abruptly involute in the postnatal period, and *Arf* is required for this process. It seemed unlikely that cell-intrinsic responses to oncogenic signals would explain this restricted expression pattern.

As we explored candidate factors that might control *Arf*, we focused on members of the Transforming growth factor β (Tgfβ) family. Tgfβs were initially identified in mammalian fibroblasts transformed with murine or feline sarcoma viruses and in cultured human melanoma cell lines as proteins that alter fibroblast morphology, and promote proliferation and growth in soft agar (De Larco and Todaro, 1978; Marquardt et al., 1983; Marquardt et al., 1984). The three mammalian Tgfβs transduce signals through a heteromeric complex containing type I and II Tgfβ receptor serine/threonine kinases (TβrI and TβrII; Tgfbr1 and Tgfbr2, respectively – Mouse Genome Informatics); binding of Tgfβ to the receptor complex activates a variety of pathways via both Smad-dependent and Smad-independent signals (Bierie and Moses, 2006; Derynck and Zhang, 2003; Massague et al., 2000). Among their effects is the capacity to arrest cell proliferation and block cancer progression, which appears to contrast the original observations. Of the three members in this family, Tgfβ2 was the most interesting because both $Arf^{+/-}$ (McKeller et al., 2002; Martin et al., 2004) and $Tgfb2^{-/-}$ (Saika et al., 2001; Sanford et al., 1997) mice display primary vitreous hyperplasia during embryonic development. We investigated the possible relationship between Tgfβ2 and *Arf* using complementary cell culture-based models and in vivo models.

MATERIALS AND METHODS

Mice and cell lines

Mice in which *Arf* exon 1β was inactivated (Kamijo et al., 1997) or replaced by a reporter gene encoding green fluorescence protein (Gfp) (Zindy et al., 2003) or encoding β-galactosidase (made in essentially the same way, A.C.M. and S.X.S., see Fig. S5 in the supplementary material) were maintained in a mixed C57BL/6 × 129/Sv genetic background. $Tgfb2^{+/-}$ mice (Sanford et al., 1997) were purchased from Jackson Laboratories. Primary MEFs from wild-type and $Arf^{+/-}$ mice were cultivated as previously described (Zindy et al., 1997). Animal studies were approved by the St Jude Children's Research Hospital and the University of Chicago Animal Care and Use Committees.

Histology studies

For in vivo studies, tissue was harvested from euthanized mice and fixed for 4 hours in 1% formaldehyde, 0.2% glutaraldehyde, 0.2% NP-40 and 0.1% SDS; washed in PBS; and stained in 1 mg/ml X-gal, 5 mM $K_3Fe(CN)_6$, 5

[1]Department of Oncology, St Jude Children's Research Hospital, Memphis, TN 38105, USA. [2]Department of Pediatrics and [3]Department of Surgery, University of Chicago, Chicago, IL 60637, USA. [4]Children's Cancer Center of Lebanon, American University of Beirut Medical Center, Beirut 1107 2020, Lebanon.

*These authors contributed equally to this work
†Author for correspondence (e-mail: sskapek@peds.bsd.uchicago.edu)

Accepted 14 April 2009

mM $K_4Fe(CN)_6$, 2 mM $MgCl_2$, 0.2% NP-40 and 0.1% SDS overnight at 30°C. Tissue was then photographed or processed for either cryostat or microtome sections, used for hematoxylin and eosin (H&E) or immunofluorescence staining for specific proteins.

Gfp, $p19^{Arf}$, Pdgfrβ and TβrII were detected by immunostaining mouse tissue as previously described (Silva et al., 2005) using rabbit anti-Gfp (A6455, Molecular Probes); rat anti-$p19^{Arf}$ (Bertwistle et al., 2004) (provided by C. J. Sherr); goat anti-Pdgfrβ (AF1042, R&D Systems); goat anti-TβrII (SC 33931, Santa Cruz); rabbit anti-phosphoserine 465/467 Smad2 (3849, Chemicon); and species-specific secondary antibodies.

Cell density in the primary vitreous was assessed using ImagePro Plus software as follows: digital photomicrographs of H&E-stained sections were used to select an area of interest (AOI) encompassing the entire posterior chamber (see Fig. S1 in the supplementary material). The number of pixels within this AOI was noted. Next, all cells (excluding erythrocytes) within the AOI were highlighted, and the number of highlighted pixels was calculated. The cellularity was then determined by dividing the cell pixel number by the total pixel number in the AOI, and it was presented as a percentage. Staining for Ki67 (Mki67 – Mouse Genome Informatics) and TUNEL labeling were performed and quantified such that the number of stained cells was normalized to the vitreous area, determined using ImagePro Plus software as previously described (Silva et al., 2005). The average area of the vitreous in midline sections used in the quantitative studies was the same in wild-type and $Tgfb2^{-/-}$ eyes at this point: 1.48×10^5 versus 1.66×10^5 pixels, respectively (P=0.537).

Stained embryos or slides were photographed using an Olympus BX60 microscope equipped with a SPOT RT Slider camera (Diagnostic Instruments) or using a Zeiss 510 NLO multiphoton/confocal laser scanning microscope.

Cell culture studies

Wild-type and $Arf^{+/-}$ MEFs (passage 2) were treated in parallel 1 day following plating, with or without Tgfβ2 (0, 1, 5, 10 ng/ml), Tgfβ1 (5 ng/ml), Pdgfb (50 ng/ml) or an equivalent volume of the relevant vehicle for 24, 48 and 72 hours, at which times cells were harvested for protein or RNA extraction, or cell cycle analysis. Cycloheximide (100 μM, Sigma) and SB431542 (10 μM, Tocris Cookson) were used in some studies.

Protein extraction and immunoblotting were performed essentially as described (Zindy et al., 1998) using 4-12% gradient gels (XCell II electrophoresis apparatus, Novex, San Diego, CA, USA) and the following primary antibodies: rabbit anti-$p19^{Arf}$ (ab80, Abcam, UK); anti-phosphoserine 465/467 (CS3101, Cell Signaling Technology); or goat anti-Hsc70 (Hspa8 – Mouse Genome Informatics; K-19, Santa Cruz Biochemicals, CA, USA) to control for protein loading. $Arf^{-/-}$ 10T1/2 cells, transduced with *Gfp*- or *Arf*-encoding retrovirus (Silva et al., 2005), were included as negative and positive controls.

Total RNA extraction and cDNA preparation were accomplished using RNeasy (Qiagen) and Superscript III RT (Invitrogen, MD, USA) according to the manufacturer's recommendations. Quantitative RT-PCR (qRT-PCR) was performed using the TaqMan ABI PRISM 7700 Sequence Detection System (Applied Biosystems, CA, USA) and gene-specific primers for *Arf:* 5′-TGAGGCTAGAGAGGATCTTGAG-3′ (forward); 5′-CGTTGCCC-ATCATCATCAC-3′ (reverse); and 5′-CGTTGCCCATCATCATCAC-3′ (qRT probe) [designed using the Primer Expression program (Applied Biosystems)]. *Gapdh* primers and probes were purchased from Applied Biosystems. Primers and probes were used at 200 nM and 50 nM, respectively. RT-PCR reactions were shown to amplify single bands by agarose gel electrophoresis. QRT-PCR data are from three replicate experiments.

LacZ expression in MEFs, prepared and cultivated as previously described (Zindy et al., 1997), was assessed using X-gal staining (see above) following fixation in 0.5% glutaraldehyde, or by measuring β-galactosidase activity in cell lysates prepared by sequential freeze/thaw in 0.25 M Tris pH 7.8, using Galacto-Light Plus (PE Biosystems).

For cell cycle analyses, cells were incubated with BrdU, harvested with trypsin/EDTA, fixed, permeabilized and costained using anti-BrdU antibody (Sigma) followed by FITC-coupled anti-mouse antibody (DAKO) and propidium iodide (Sigma; 10 μg/ml) and analyzed using either a FACScan or FACSCalibur (BD Biosciences, San Jose, CA, USA). Relative cell cycle change represents the percent difference in the fraction of Tgfβ2-treated cells in a particular phase as compared with vehicle treated cells.

Chromatin immunoprecipitation

$Arf^{lacZ/lacZ}$ MEF cells (3×10^6/immunoprecipitation) treated with Tgfβ2 (5 ng/ml) or vehicle for 1.5 hours were crosslinked, sonicated and immunoprecipitated with anti-Smad2/3 antibody (sc6033, Santa Cruz) or IgG (AB-108-C, R&D Systems) as a control. Protein A/G sepharose beads (sc2003, Santa Cruz) were used to collect the protein-chromatin complexes. The beads were washed sequentially with low salt, high salt, LiCl and TE buffers (Upstate ChIP Kit, Millipore) and eluted in 0.1 M $NaHCO_3$, 1% SDS. Crosslinking was reversed by incubation at 67°C overnight and the genomic DNA was extracted with a Qiagen PCR Purification Kit. A total of 3% of the precipitated DNA and 1% input DNA was amplified by PCR using primer sets for *Id1* and different regions of *Arf* (primer sequences are available upon request). The PCR products were resolved on 1.5 % agarose gels and stained with ethidium bromide.

Quantitative and non-quantitative studies

All quantitative studies were accomplished using three or more samples from separate animals, or three or more separate cell culture experiments. Non-quantitative results from histological studies are representative of findings using at least three embryos of the indicated genotypes, obtained from two or more separate experiments. Statistical significance of any quantitative differences was assessed by Student's *t*-test.

RESULTS

Ocular defects in *Tgfb2*$^{-/-}$ embryo eyes

Currently, the only established developmental activity of $p19^{Arf}$ is to control the accumulation of cells within the vitreous (Silva et al., 2005). If it acted with Tgfβ2 during this process, we reasoned that the developmental defects in the absence of *Arf* should parallel those in $Tgfb2^{-/-}$ embryos. Without *Arf*, increased numbers of vitreous cells are detectable at embryonic day (E) 13.5, approximately 1 day after its expression is evident (Silva et al., 2005). At that point, there is excess proliferation in the vitreous, a defect that is intrinsic to the *Arf*-expressing cells (Thornton et al., 2007). Notably, *Arf* loss does not measurably change the small number of apoptotic cells (Silva et al., 2005). Like $Arf^{-/-}$ mice, $Tgfb2^{-/-}$ mice displayed obvious primary vitreous hyperplasia at E18.5 and at birth, whereas $Tgfb2^{+/-}$ and $Tgfb2^{+/+}$ eyes were normal (Fig. 1A; see Fig. S2 in the supplementary material). Quantitative analyses of younger embryos revealed increased cell density in the primary vitreous of $Tgfb2^{-/-}$ versus wild-type embryos as early as E13.5, and this was associated with increased cell proliferation (Fig. 1A,B; see Fig. S3 in the supplementary material). As in $Arf^{-/-}$ embryos (Silva et al., 2005), the average percentage of apoptotic cells (3.1±3.8% versus 2.5±2.1%, n=~350 cells counted for each genotype, P=0.81) was similar in the presence or absence of Tgfβ2, respectively. Proliferation continued in the hyperplastic primary vitreous of $Arf^{-/-}$ and $Tgfb2^{-/-}$ embryos at E18.5 (Fig. 1C). Lastly, nearly all of the hyperplastic vitreous cells expressed Pdgfrβ in $Tgfb2^{-/-}$ embryos (Fig. 1D), again mimicking the findings in $Arf^{-/-}$ embryos (Silva et al., 2005). Hence, loss of *Tgfb2* causes hyperplastic expansion of Pdgfrβ-expressing cells from early stages of primary vitreous formation, as in $Arf^{-/-}$ embryos.

Relationship between Tgfβ2 and $p19^{Arf}$ in MEFs

To begin to address whether *Tgfb2* could lie 'upstream' of *Arf* in a linear pathway, we explored how the presence or absence of *Arf* influenced mitogenic or anti-mitogenic effects of Tgfβ in cultured MEFs. Exposure of wild-type MEFs to Tgfβ2 for 24 and 72 hours decreased the fraction of cells in S phase by 15-25% (Fig. 2A, lanes 5 and 7). This was balanced by increases in the G_0/G_1 fraction at

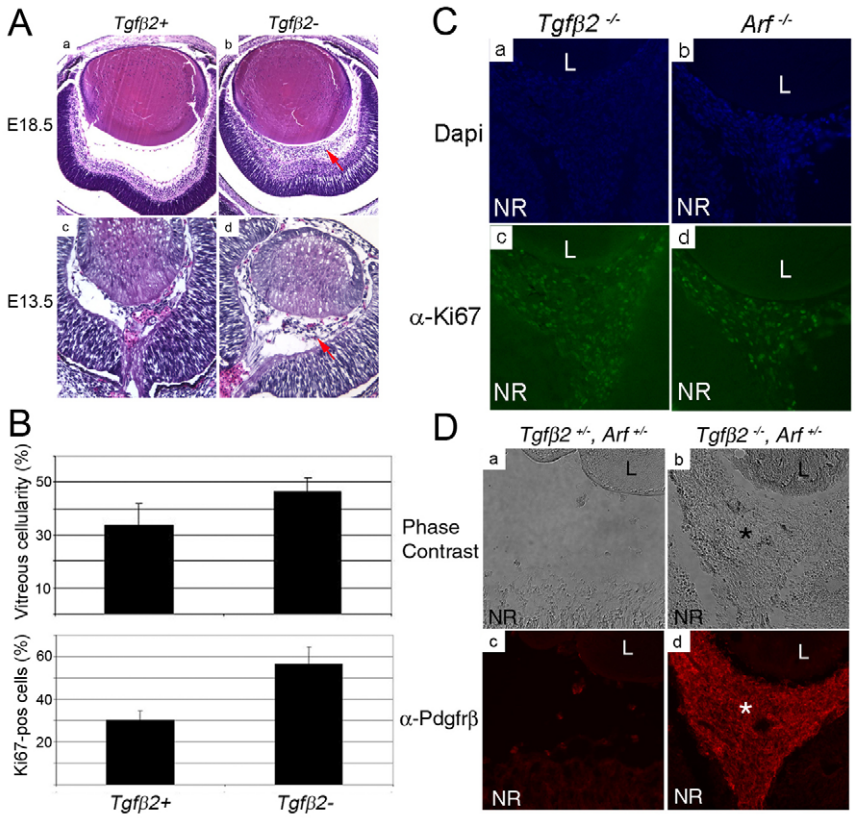

Fig. 1. Primary vitreous hyperplasia in *Tgfb2*$^{-/-}$ eyes resembles the *Arf*$^{-/-}$ phenotype. (**A**) Photomicrographs of H&E-stained eyes taken from phenotypically normal *Tgfb2*$^{+/-}$ and *Tgfb2*$^{-/-}$ mice at E18.5 (a,b) and E13.5 (c,d). Vitreous hyperplasia (arrow) increases from E13.5 to E18.5 in *Tgfb2*$^{-/-}$ mice. (**B**) Quantitative analyses show that the percentage cellularity in the vitreous (top) and the percentage of cells that express Ki67 (bottom) are increased in *Tgfb2*$^{-/-}$ (*Tgfβ2*-) embryos at E13.5 as compared with wild type (*Tgfb2*$^{+/-}$ and *Tgfb2*$^{+/+}$ pooled; *Tgfβ2*+) (P=0.011 and P<0.001, respectively). (**C**) Representative photomicrographs of immunofluorescence-stained eyes from E18.5 embryos of the indicated genotype showing Ki67-positive, proliferating cells (green) in the retrolental mass between the lens (L) and the neuroretina (NR). Nuclei are stained with DAPI (blue). (**D**) Representative phase contrast and immunofluorescence images of *Tgfb*$^{+/-}$ *Arf*$^{+/-}$ (a,c) and *Tgfb2*$^{-/-}$ *Arf*$^{+/-}$ (b,d) embryos showing that hyperplastic vitreous cells (*) between the lens (L) and neuroretina (NR) expressed Pdgfrβ in *Tgfb2*$^{-/-}$ *Arf*$^{+/-}$ embryos.

both times and in the G_2/M fraction at 24 hours (Fig. 2A, lanes 1, 3 and 9). Tgfβ2-dependent changes in *Arf*$^{-/-}$ MEFs paralleled those in wild-type cells at 24 hours (Fig. 2A, compare lanes 1 and 2; 5 and 6; 9 and 10). However, the pronounced block of cells in S phase and the accumulation of cells in G_1 at 72 hours were not maintained without p19^{Arf} (Fig. 2A, compare lanes 3 and 4; 7 and 8; 11 and 12). The requirement for *Arf* correlated with p19^{Arf} induction by Tgfβ2 at 48 and 72 hours (Fig. 2B, lanes 2 and 3 versus lane 1; see Fig. S4A in the supplementary material); p19^{Arf} was not induced at 24 hours (see Fig. S4B in the supplementary material). The ability of p19^{Arf} to maintain Tgfβ2-driven growth arrest may depend on p53 (Trp53 – Mouse Genome Informatics), which cooperates with Tgfβ1 to control proliferation in MEFs (Cordenonsi et al., 2003). However, we did not observe *Arf*-dependent induction of p21^{Waf1} (Cdkn1a – Mouse Genome Informatics), a well-described p53 target, or other Cdk inhibitors (see Fig. S4A in the supplementary material). Moreover, *p21*$^{-/-}$ mice did not display vitreous hyperplasia (see Fig. S4C in the supplementary material), and it is hence not the main Tgfβ2 target in the eye.

Mechanistic studies in MEFs

We investigated the mechanistic aspects of Tgfβ2-driven p19^{Arf} induction. We first explored whether p19^{Arf} induction correlated with increased *Arf* mRNA and promoter activity. The latter was addressed using a new reporter mouse, in which *Arf* exon 1β was replaced by *lacZ* cDNA encoding the β-galactosidase reporter; X-gal staining in the mouse recapitulated the previously described *Arf* expression in the eye and the testis (Fig. 2C; see Fig. S5 and Fig. S6A,B in the supplementary material). Like Gfp expression in the *Arf*$^{Gfp/+}$ mouse (Martin et al., 2004; Zindy et al., 2003), β-galactosidase activity increased as *Arf*$^{lacZ/lacZ}$ MEFs were cultivated using a 3T9 protocol (see Fig. S6C in the supplementary material), and as they grew more confluent (Fig. 2D, lanes 2, 5, 8), paralleling previous findings with native p19^{Arf} (Kamijo et al., 1997; Sharpless et al., 2004). We observed that Tgfβ2 increased *Arf* mRNA in wild-type MEFs and *Arf* promoter transcription in *Arf*$^{lacZ/lacZ}$ MEFs at 72 but not 24 hours, correlating with changes at the protein level (Fig. 2D, lanes 8 and 10 versus 2 and 4; see Fig. S7A in the supplementary material), although the reporter detected *Arf* induction earlier than the qRT-PCR assay. Lastly, p19^{Arf} expression fell following cycloheximide exposure in Tgfβ2-treated MEFs at least as rapidly as in the control (see Fig. S7B in the supplementary material). Hence, Tgfβ2 controls p19^{Arf} expression by inducing its promoter without measurably changing the stability of the protein.

Next we addressed whether Tgfβ1 or platelet derived growth factor B (Pdgfb) shared the capacity to induce *Arf* in MEFs. The former was tested because it can reverse primary vitreous hyperplasia in *Tgfb2*$^{-/-}$ mice (Zhao and Overbeek, 2001), whereas the latter acts as a potent mitogen in MEFs (Silva et al., 2005). All of the effects of Tgfβ1 on *Arf* expression paralleled those of Tgfβ2 (Fig. 2D, lanes 3, 6, 9 versus 4, 8, 10; see Fig. S7A in the supplementary material). By contrast, Pdgfb did not induce the reporter at 48 or 72 hours (Fig. 2D, lanes 12 and 13; negative data not shown). Therefore, *Arf* induction in this cell culture model does not simply represent a response to supraphysiological mitogens.

The role of Smad proteins

We also tested if the observed effects depended on Smad2 because this signaling protein was phosphorylated in response to Tgfβ2 in MEFs (Fig. 2E). To test this, we exposed the cells to SB431542, an inhibitor of TβrI (Seay et al., 2005). This chemical inhibited Smad2 phosphorylation at serine 465/467 and blocked both p19^{Arf} and β-galactosidase induction in wild-type and *Arf*$^{lacZ/lacZ}$ MEFs, respectively (Fig. 2F,G). We also used a genetic approach to exclude

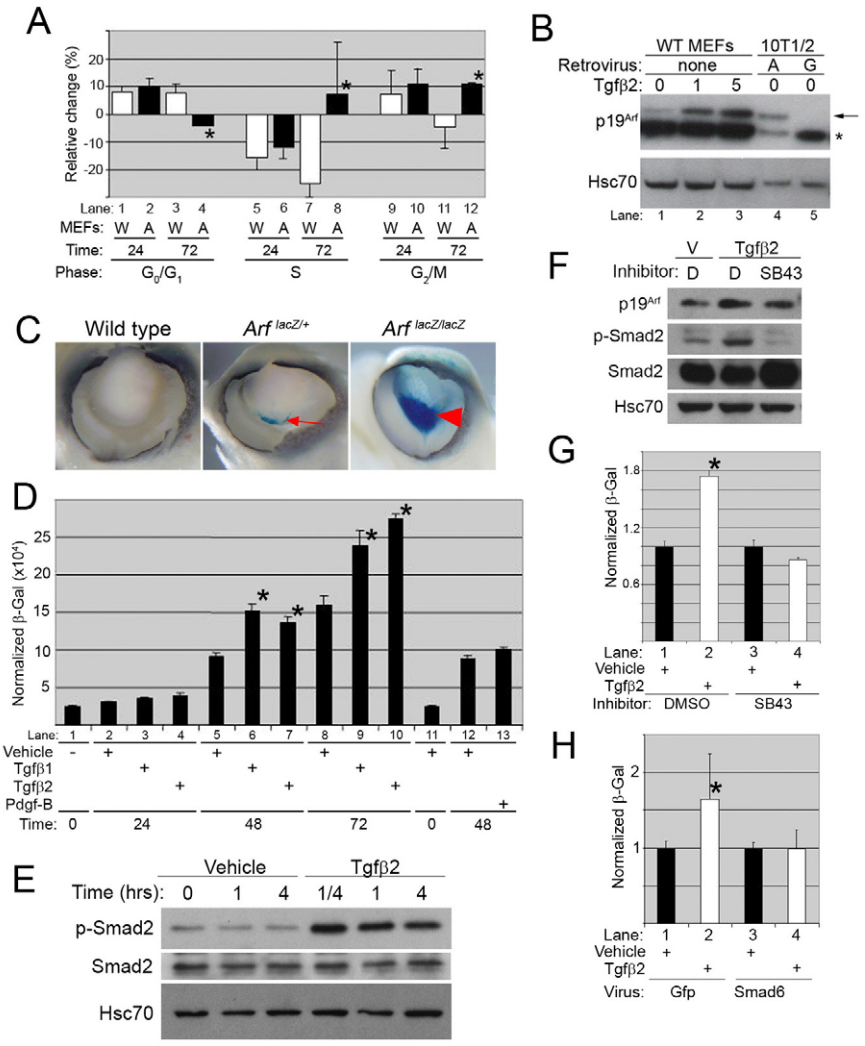

Fig. 2. Tgfβ activates the *Arf* promoter in a Smad-dependent manner. (**A**) Relative changes in cell cycle phases in wild-type (W) and $Arf^{-/-}$ (A) MEFs. Data represent the average change (and standard deviation) in cell cycle phase in Tgfβ2 (5 ng/ml) treated cells expressed as percentage increase or decrease from vehicle-treated cells at 24 or 72 hours. Asterisk (*) denotes the statistically significant differences between wild-type and $Arf^{-/-}$ MEFs (P<0.048 at each point). (**B**) Western blot for $p19^{Arf}$ or Hsc70 as a loading control in wild-type MEFs exposed to 1 or 5 ng/ml Tgfβ2 for 72 hours, and in *Arf*-deficient 10T1/2 cells transduced with *Arf*- (A) or *Gfp*-encoding (G) retrovirus as a control. Arrow, $p19^{Arf}$; asterisk (*), a crossreactive protein. (**C**) Representative whole-mounted, E13.5 embryo eyes from mice of the indicated genotype, following X-gal staining. Note that *Arf*-expressing cells (arrow) are greatly expanded in the $Arf^{lacZ/lacZ}$ embryo (arrowhead). (**D**) β-Galactosidase activity in $Arf^{lacZ/lacZ}$ MEFs treated with the indicated growth factors. Data represent average enzyme activity, normalized to protein quantity. Statistically significant differences (P<0.005) between Tgfβ2- and vehicle-treated MEFs are marked (*). (**E**) Western blots for the indicated proteins in wild-type MEFS show that Smad2 is phosphorylated after exposure to 5 ng/ml Tgfβ2 for the indicated times. (**F**) Western blots for the indicated proteins show that SB431542 (SB43, a TβrI inhibitor) impeded Smad2 phosphorylation and $p19^{Arf}$ induction after Tgfβ2 (5 ng/ml, 48-hour treatment) in wild-type MEFs. V, vehicle (for Tgfβ2); D, DMSO (vehicle for SB431542). Note that the crossreactive protein (*, B) is not detected using a later antibody batch. (**G**) β-Galactosidase activity in $Arf^{lacZ/lacZ}$ MEFs exposed to SB431542 (SB43) in addition to Tgfβ2 (5 ng/ml) or vehicle for 48 hours. Data represent average enzyme activity, normalized to protein quantity, relative to vehicle-treated cells. Statistically significant differences (P<0.005) between Tgfβ2- and vehicle-treated MEFs are marked (*). (**H**) β-Galactosidase activity in $Arf^{lacZ/lacZ}$ MEFs transduced with *Gfp*- or *Smad6*-expressing adenovirus and treated with Tgfβ2 (5 ng/ml) for 48 hours. Data represent average enzyme activity, normalized to protein quantity, relative to vehicle-treated. Statistically significant differences (P<0.005) between Tgfβ2- and vehicle-treated MEFs are marked (*).

the possibility that this might represent an off-target effect of the chemical. The ectopic expression of the inhibitory Smad6 (Derynck and Zhang, 2003) impeded *Arf* promoter activation by Tgfβ2 (Fig. 2H), proving that Smad-dependent signals stemming from the Tgfβ receptor drive $p19^{Arf}$ expression.

Next, we considered whether Smads directly influence the *Arf* promoter because multiple potential Smad binding elements (SBEs) flank *Arf* exon 1β (Fig. 3C). Chromatin immunoprecipitation (ChIP) using an antibody recognizing Smad2 and Smad3 is described to show Smad binding at promoters like that driving mouse *Id1* expression (Smith et al., 2009). In our experiments, Smad2/3 binding was evident at baseline levels and it increased 1.5 hours following exposure of $Arf^{lacZ/lacZ}$ MEFs to Tgfβ1 (Fig. 3A). To interrogate the *Arf* gene, we designed 12 PCR primer sets spanning the –2.2 kb to +1.1 kb region flanking exon 1β (Fig. 3B,C; primer sequences are available upon request). ChIP assay shows that

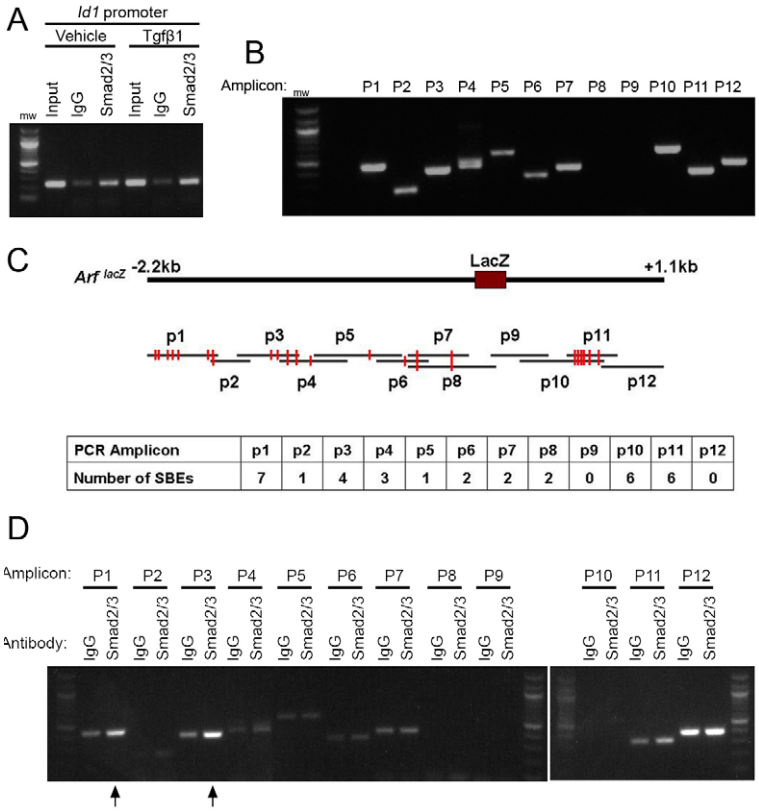

PCR Amplicon	p1	p2	p3	p4	p5	p6	p7	p8	p9	p10	p11	p12
Number of SBEs	7	1	4	3	1	2	2	2	0	6	6	0

Fig. 3. Tgfβ promotes Smad2/3 binding to the *Arf* promoter. (**A**) Representative chromatin immunoprecipitation (ChIP) with control (IgG) or anti-Smad2/3 antibody using chromatin isolated from $Arf^{lacZ/lacZ}$ MEFs following exposure to vehicle or Tgfβ1 (5 ng/ml) for 1.5 hours. Immunoprecipitated DNA and input DNA were amplified by PCR using *Id1*-specific primers. (**B**) Representative photo of ethidium bromide-stained agarose gel showing PCR products from 12 primer pairs spanning 3 kb of the *Arf* gene as indicated in C. This gel represents sheared chromatin input from Tgfβ1-treated $Arf^{lacZ/lacZ}$ MEFs used in A and D. Note that primers are complementary to the wild-type *Arf* locus, so primer pair 8 and 9 fails to amplify a product from the targeted allele. (**C**) Schematic diagram of the mouse *Arf* gene in the $Arf^{lacZ/lacZ}$ mouse and the PCR amplicons used for ChIP. Red vertical lines represent putative SBEs. (**D**) Representative photo of gel following electrophoresis of ChIP products from $Arf^{lacZ/lacZ}$ MEFs used in A. Arrows indicate Smad2/3 binding to amplicons 1 and 3.

Smad2/3 binding was observed at amplicons 1 and 3 proximal to the first exon in $Arf^{lacZ/lacZ}$ MEFs 1.5 hours following the addition of Tgfβ1 (Fig. 3C,D). Binding at amplicons 2 and 4 was also observed, but the signal was weaker. Selective Smad2/3 binding to the chromatin was not convincing at other regions, including those with putative SBEs. Interestingly, the relatively small amount of binding observed at amplicon 2 suggests that Smad2/3 might bind to two distinct regions in amplicons 1 and 3. Thus, although increased *Arf* expression was not readily detected until 48 hours following the addition of either Tgfβ1 or 2, increased Smad2/3 binding is present in the *Arf* promoter shortly after Tgfβ exposure.

Tgfβ2 controls *Arf* expression in the mouse eye

We felt it was important to verify that our findings in MEFs were relevant to *Arf* regulation in the mouse eye. Immunofluorescence staining detects $p19^{Arf}$ in subnuclear foci in the mouse testis (Bertwistle et al., 2004). $p19^{Arf}$ was similarly detected in vitreous cells in $Tgfb2^{+/+}$ and $Tgfb2^{+/-}$ embryos at E13.5, but not in the $Tgfb2^{-/-}$ littermates stained in parallel (Fig. 4A). To determine whether decreased $p19^{Arf}$ represented decreased transcription in vivo, we employed $Arf^{Gfp/+}$ and $Arf^{lacZ/+}$ reporter mice. As expected, vitreous hyperplasia developed at E15.5 in $Arf^{Gfp/Gfp}$ embryos that were heterozygous for *Tgfb2*, and nearly all of the vitreous cells expressed the *Arf* promoter (Fig. 4B, panels a and b), consistent with our observations in $Arf^{lacZ/lacZ}$ embryos (Fig. 2C). Hyperplasia was also evident in $Arf^{Gfp/Gfp}$ $Tgfb2^{-/-}$ embryos (Fig. 4B, panel c) (formally establishing that Tgfβ2 does not provide essential mitogenic signals to drive vitreous hyperplasia), but Gfp staining showed *Arf* promoter activity to be markedly decreased (Fig. 4B, panel d). Similar observations using $Tgfb2^{-/-}$ $Arf^{lacZ/+}$ embryos at E13.5 (Fig. 4C) proved that the effects of Tgfβ2 on *Arf* expression were not specific to a single reporter and did not depend on an *Arf*-deficient state. Consistent with potentially direct signaling, immunofluorescence staining revealed that Gfp and TβrII expression overlapped in some of the vitreous cells of $Arf^{Gfp/+}$ embryos (Fig. 4D). Furthermore, phosphoSmad2 was present in nuclei in the primary vitreous in E13.5 wild-type embryos and throughout the retrolental mass in newborn $Arf^{-/-}$ mice (Fig. 4E; additional data not shown). Because essentially all of the cells in the retrolental mass expressed the *Arf* gene in the embryo (Fig. 4B) and in the newborn period (Martin et al., 2004), we conclude that Tgfβ2 directly impacts cells expressing *Arf*.

Tgfβ2 controls *Arf* expression at other embryonic sites

Finally, a survey of the $Arf^{lacZ/+}$ embryos revealed two new sites where *Arf* is expressed during development: within the stroma of the developing cornea at E12.5 and E13.5 (Fig. 5Aa,b) and around the umbilical arteries within the abdominal/pelvic cavities between E13.5 through to the early postnatal period (Fig. 5C; see Fig. S8A in the supplementary material). Expression in the cornea stroma at this stage is interesting because Tgfβ2 induces extracellular matrix proteins such as collagen I and lumican, enhancing cornea thickness (Saika et al., 2001). However, there is no obvious thinning in the $Arf^{-/-}$ cornea (see Fig. S9 in the supplementary material). *Arf* expression in the umbilical arteries, which are essential only during embryo development (like the hyaloid vasculature), parallels the pattern in the vitreous in that the cells are perivascular in location and some coexpress Pdgfrβ (Fig. 5Cc; see Fig. S8B in the supplementary material). However, aspects of umbilical artery biology appeared unaffected by *Arf* loss. For example, the atresia that typically develops in the left umbilical artery between E13.5 and E14.5 (Warot et al., 1997) still occurs without $p19^{Arf}$ (Fig. 5Cb). In both the cornea and the umbilical arteries, absence of Tgfβ2 diminished *Arf* expression (Fig. 5Ac,d; Fig. 5B,D). Although the functional relevance of this

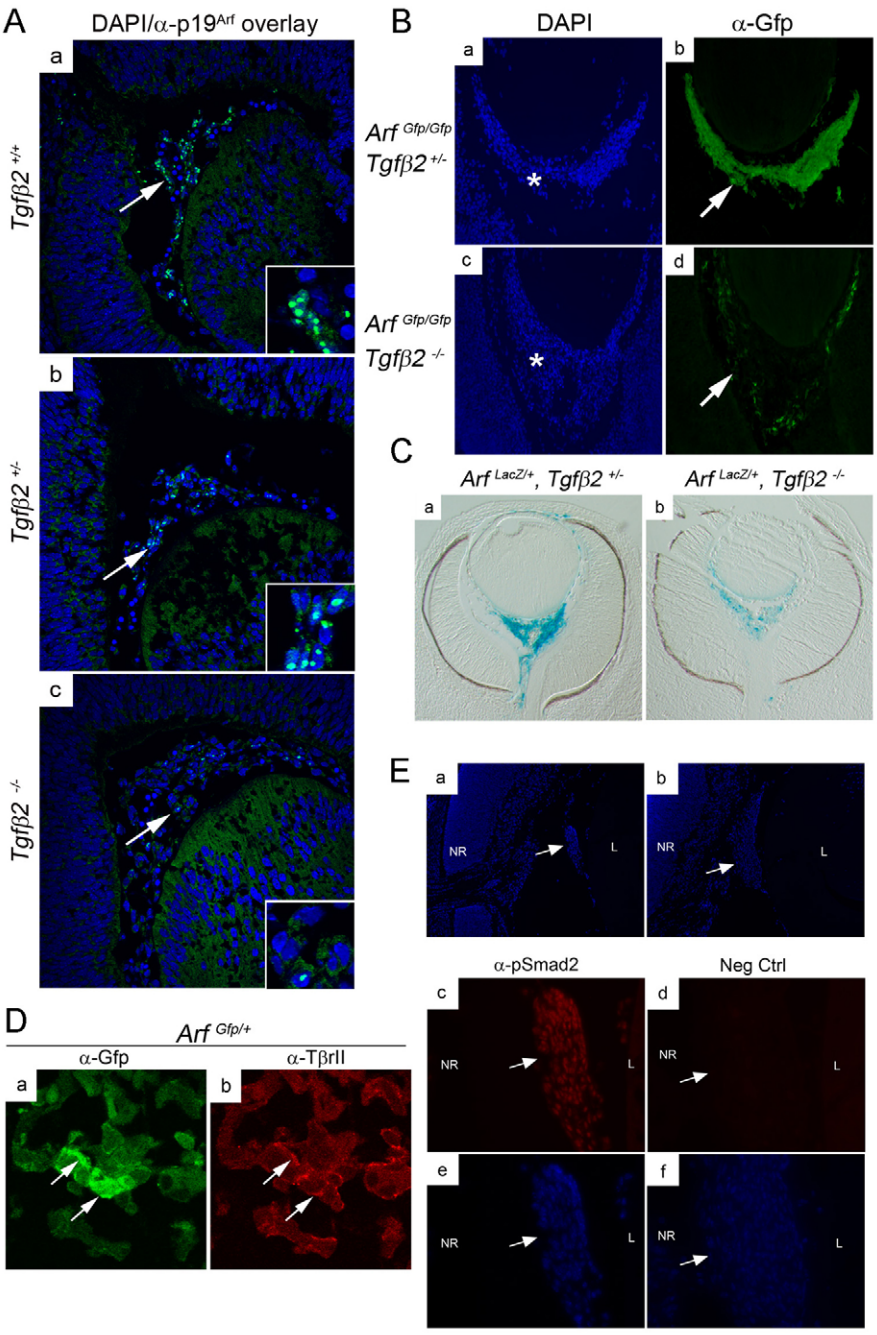

Fig. 4. *Tgfb2* fosters *Arf* expression in the primary vitreous. (**A**) Representative photomicrographs of eyes from E13.5 mouse embryos stained with DAPI (blue) and anti-p19^{Arf} (green). Arrows show p19^{Arf}-positive vitreous cells that are digitally magnified in insets. Genotypes are as indicated. (**B**) Representative photomicrographs of eyes from E15.5 mouse embryos stained with DAPI or anti-Gfp. Asterisk (*) indicates hyperplastic vitreous cells that did or did not express *Arf* (arrows). (**C**) Photomicrographs of paraffin sections through X-gal-stained E13.5 embryo eyes of the indicated genotypes. (**D**) Representative photomicrographs of eyes from E13.5 mouse embryos stained with anti-Gfp (green) or anti-TβrII (red). Arrows show that some *Arf*-expressing cells also express TβrII. (**E**) Representative photomicrographs of eyes from postnatal day 1 mouse eye stained anti-phosphoSmad2 or negative control lacking the primary antibody, which was detected using rhodamine-coupled secondary antibody (red). DAPI-stained (blue) images show the retrolental mass (arrow) between the lens (L) and neuroretina (NR) in the *Arf*$^{-/-}$ mouse, shown at 100× (a,b) and 400× (c-f) original magnification.

pathway in umbilical artery and cornea development is not yet clear, we can confidently conclude that Tgfβ2-mediated control of *Arf* promoter activity extends beyond the vitreous of the eye.

DISCUSSION

The clear role that *Arf* plays in mouse development implies that its control must extend beyond that provided by the deregulated signals accompanying the activation of certain oncogenes. Whereas this regulatory paradigm focuses on cell-intrinsic signaling, our findings provide the first evidence that *Arf* expression can be controlled by specific cell-extrinsic signals from Tgfβ2 during development and in MEFs. We can now begin to integrate our findings with emerging knowledge regarding the regulation of p19^{Arf} (Gil and Peters, 2006; Kim and Sharpless, 2006).

First, although there is some evidence that its expression is controlled by post-transcriptional mechanisms (Colombo et al., 2005), our findings using two different reporter systems indicate that the Tgfβ-dependent induction depends largely, and perhaps exclusively, on transcriptional activation. Unfortunately, regulatory mechanisms guiding transcription of *Arf* and the flanking *Ink4a* (*Cdkn2a* – Mouse Genome Informatics) and *Ink4b* (*Cdkn2b* – Mouse Genome Informatics) genes are complex and incompletely understood. The activity of certain Polycomb group proteins (notably Bmi1) leads to the methylation and silencing of *Arf*, *Ink4a* and to a lesser extent *Ink4b* in MEFs (Jacobs et al., 1999). In the developing mouse, the relative importance of Bmi1-mediated repression of specific genes at this locus is cell type-dependent (Bruggeman et al., 2005; Molofsky et al., 2005). The entire

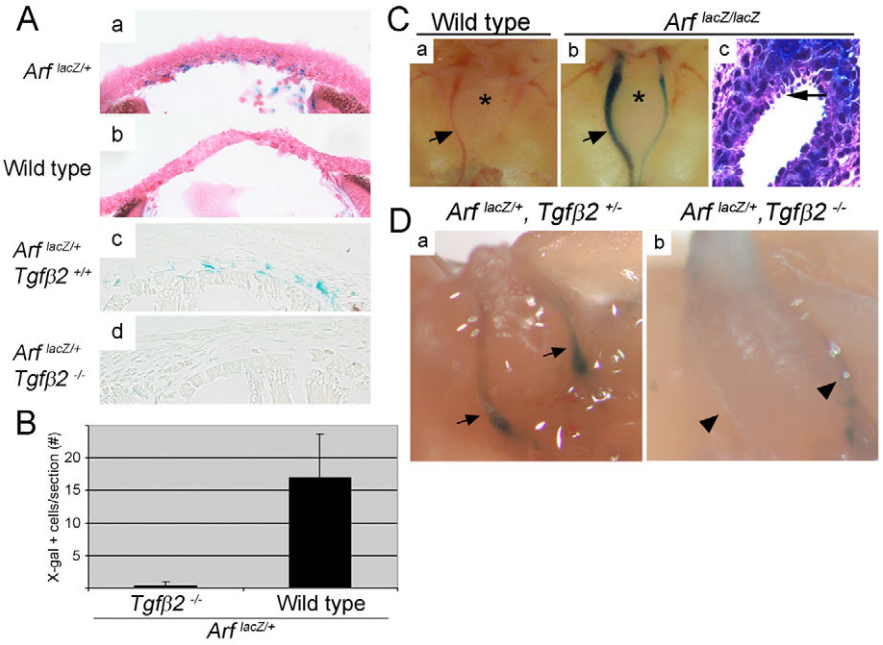

Fig. 5. *Tgfb2* is required for *Arf* expression in the embryonic cornea and umbilical arteries. (**A**) Photomicrographs of sections through the cornea in E13.5 mouse embryos of the indicated genotypes and stained with X-gal with (a,b) or without (c,d) Eosin. (**B**) Quantitative analysis showing that the number of X-gal-positive cells across the cornea from midline sections of eyes is higher in phenotypically normal (wild-type) E13.5 $Arf^{lacZ/+}$ $Tgfb2^{+/+}$ and $Arf^{lacZ/+}$ $Tgfb2^{+/-}$ embryos, as compared with $Arf^{lacZ/+}$ $Tgfb2^{-/-}$ embryos (P=0.0004). (**C**) Photomicrographs of X-gal-stained umbilical artery (arrows) adjacent to urinary bladder (*) in E14.5 mouse embryos of the indicated genotype shown as whole mount (a,b) and as cross-section through the umbilical artery (c). Short arrows (a,b) indicate the right umbilical artery, whereas the left umbilical artery is much smaller at this stage. *Arf*-expressing cells (blue) are perivascular in the umbilical artery and flank endothelial cells (long arrow, c), which are not X-gal-positive. (**D**) Photomicrographs show that X-gal staining of right and left umbilical arteries in E13.5 $Arf^{lacZ/+}$ $Tgfb2^{+/+}$ embryos (arrows, a) is diminished in the absence of Tgfβ2 (arrowheads, b).

Ink4b/Arf/Ink4a locus can also be silenced by binding of the DNA replication protein Cdc6, leading to the recruitment of histone deacetylases to a regulatory domain in the *Ink4b* promoter (Gonzalez et al., 2006). Of note, neither $p16^{Ink4a}$ nor $p15^{Ink4b}$ were induced with $p19^{Arf}$ by Tgfβ2 in our model (see Fig. S4A in the supplementary material), which speaks against Tgfβ2-dependent modification of the entire gene locus. Certain other transcription factors such as Tbx2 (Jacobs et al., 2000), E2f1 and E2f3 (Aslanian et al., 2004; DeGregori et al., 1997), Dmp1 (Inoue et al., 1999) and pokemon (Zbtb7a – Mouse Genome Informatics) (Maeda et al., 2005) act on sites found close to exon 1β. Others act more remotely; for example, FoxO family members bind a regulatory element approximately 8 kb 3′ of exon 1β (Bouchard et al., 2007). Mechanisms by which other transcription factors like p53 (Kamijo et al., 1998), Myc (Zindy et al., 1998) and Twist (Maestro et al., 1999) positively or negatively regulate mouse *Arf* are even less clear. Despite the fact that our ChIP studies show Smad2/3 binding to sites flanking *Arf* exon 1β, neither Tgfβ1 nor Tgfβ2 induced a plasmid reporter containing ~2.5 kb 5′ and ~1.3 kb 3′ to exon 1β transiently transfected into mouse 10T1/2 fibroblasts [which lack *Arf* (Thornton et al., 2007)], and into WT MEFs (negative data not shown). These negative data might imply that *Arf* induction is mediated by mechanisms that are not reflected in a transiently expressed reporter. They could also indicate that Smad-dependent changes near the promoter must cooperate with other cis regulatory elements that are further removed from the promoter.

Another important mechanistic issue relates to exactly how Tgfβ2 signals get to the *Arf* promoter. We have some insights, which are as follows: first, our detection of both TβrII and phosphoSmad2 in *Arf*-expressing cells in vivo indicates that Tgfβ2 signaling can directly impact the cells that express the *Arf* promoter; second, because *Arf* induction correlates with Smad2 phosphorylation and can be blocked by chemical inhibition of TβrI and the ectopic expression of Smad6, it seems safe to conclude that a Smad-dependent process is required in MEFs; lastly, our ChIP assay using a Smad2/3-specific antibody showed that Smad proteins directly bind to the *Arf* gene. That Smad2 phosphorylation is detected in *Arf*-expressing cells in the embryo suggests but does not prove it to be the crucial Smad in vivo. Its candidacy is strengthened by the fact that $Smad3^{-/-}$ mice, which are viable, appear to have normal eyes (Banh et al., 2006; Zhu et al., 1998). Formally evaluating the role of Smad2 may require its knockout in cells destined to express the *Arf* promoter because $Smad2^{-/-}$ mice suffer early embryonic lethality (Nomura and Li, 1998; Weinstein et al., 1998). The genetically engineered mice needed to accomplish this experiment are not currently available.

Certain mechanistic facts must still be elucidated. Like in other scenarios, we suspect that Smads cooperate with other transcription factors to enhance *Arf* transcription. The region bound by Smad2/3 in our experiments contains many putative transcription factor binding sites, including potential sites for C/EBPβ (also known as Cebpβ), a known Smad-interacting protein (Ross and Hill, 2008) (TFSEARCH result; http://www.cbrc.jp/htbin/nph-tfsearch). However, its role in *Arf* regulation is not evident from the literature. The rapid localization of Smad2/3 to the promoter, and the delayed increase in measurable *Arf* expression, challenges us to more broadly consider the role Smads might play in this process. For example, Smad binding might initiate a cascade of events that make the chromatin more accessible to other transcriptional activators,

even those like FoxO that act at a distance. As such, gaining insight into the Tgfβ-dependent changes in DNA methylation and histone status is likely to be informative. Lastly, although Smad2/3 binding to the promoter is detectable, given the fact that Smad6 preferentially inhibits BMP signaling (Goto et al., 2007; Kirkbride et al., 2008), it is possible that BMPs; Smads 1, 5 and 8; and TβrIII might also contribute to *Arf* regulation.

Our findings shed light on the molecular basis for the crucial developmental process guiding the maturation of the primary vitreous into the avascular and largely acellular secondary vitreous, a developmental process that is essential for normal vision, and this might be relevant to human eye disease. We previously established that without *Arf*, vision is severely compromised because the vitreous hyperplasia obscures the optic lens and destroys the retina (Martin et al., 2004). This ocular defect resembles severe PHPV, a disease long known to be caused by failed maturation of the primary vitreous and persistence of the hyaloid vessels (Goldberg, 1997; Haddad et al., 1978). Tgfβ2 resides upstream of *Arf* in this developmental program. Interestingly, this observation is also consistent with a recent finding that selective inactivation of TβrII using Cre recombinase expressed from a neural crest-specific promoter appears to mimic the $Arf^{-/-}$ eye phenotype (Ittner et al., 2005). Based on these mouse models, we suggest that a search for the molecular basis for the human disease should include studies of human *ARF*, *TGFB2* and the yet-to-be-defined components of the signaling pathway.

Tgfβ2 loss leads to a complex developmental phenotype that includes multiple craniofacial, cardiac, pulmonary, urogenital and skeletal defects (in addition to the ocular abnormalities mentioned here) (Sanford et al., 1997). Molecular mechanisms underlying these other defects are still elusive; certainly, the absence of these other defects in $Arf^{-/-}$ mice indicates that, unlike the primary vitreous hyperplasia, they do not arise merely due to failed induction of *Arf*. This also implies that, although Tgfβ2 is required for *Arf* expression at certain sites, it is not sufficient at others. We are taking advantage of our complementary cell culture-based model and the $Arf^{lacZ/+}$ reporter mouse to identify putative cooperating signaling proteins. More refined molecular or physiological studies will be required to determine the functional consequences of loss of *Arf* in the cornea and umbilical artery where the Tgfβ2/$p19^{Arf}$ pathway is intact but anatomic abnormalities are not apparent in the absence of *Arf*.

Beyond development and eye disease, our finding of a linear pathway between Tgfβ and $p19^{Arf}$ has potential implications for the tumor suppressor actions of these proteins. It is interesting that both Tgfβ1 and $p19^{Arf}$ block early papilloma formation triggered by DMBA/TPA in the mouse (Cui et al., 1996; Kelly-Spratt et al., 2004); however, Tgfβ1 does not hinder progression of the papilloma to an invasive cancer (Cui et al., 1996). Conceptually, anti-cancer effects of Tgfβ in this model could be a result of $p19^{Arf}$ induction, and *Arf* deletion might coincide with loss of the tumor suppressive effects of Tgfβ. Dynamic regulation of $p19^{Arf}$ at different phases of cancer development, like the sequential induction of *Arf* during Myc-driven lymphomagenesis, has been attributed to the accumulation of additional oncogenic events (Bertwistle and Sherr, 2007). Our observations support an alternative hypothesis that extracellular signals from Tgfβ, derived from either tumor cells or stroma elements, might contribute to *Arf* regulation at different stages of tumor development and progression.

We gratefully acknowledge support from the SJCRH Animal Resources Center, Transgenic and Gene Knock-out, and Scientific Imaging core resources; technical assistance by P. Chu and S. Stark; and helpful discussions with T. Abramova (University of Chicago), and M. Kastan, P. McKinnon, H. Russell, C. J. Sherr, R. Williams, F. Zindy and other members of the Kastan and Sherr laboratories (all at SJCRH). S.X.S. was supported by grants from the National Eye Institute (R01 EY014368) and the American Cancer Society (RSG 0403601-DDC) and by the American Syrian Lebanese Associated Charities (ALSAC) of SJCRH. Deposited in PMC for release after 12 months.

Author contributions

All authors contributed to experimental design and implementation and assisted with data analysis and writing; N.E.F.A. carried out experiments showing *Arf* regulation by Tgfβ in vivo, cell cycle analyses and some in vitro mechanistic studies, and wrote the first manuscript draft; Y.Z. carried out most of the in vitro mechanistic studies, including experiments proving Smad-dependence and ChIP assays; A.C.M. generated the *Arf lacZ* targeting construct, $Arf^{lacZ/+}$ mouse ES cells, and much of the phenotype analysis; S.X.S. conceived of and guided the overall project direction, assisted with experimental conduct and data analysis, and wrote final drafts of the manuscript.

Supplementary material

Supplementary material for this article is available at http://dev.biologists.org/cgi/content/full/136/12/2081/DC1

References

Aslanian, A., Iaquinta, P. J., Verona, R. and Lees, J. A. (2004). Repression of the Arf tumor suppressor by E2F3 is required for normal cell cycle kinetics. *Genes Dev.* **18**, 1413-1422.

Banh, A., Deschamps, P. A., Gauldie, J., Overbeek, P. A., Sivack, J. G. and West-Mays, J. A. (2006). Lens-specific expression of Tgf-b induces anterior subcapsular cataract formation in the absence of Smad3. *Invest. Ophthalmol. Vis. Sci.* **47**, 3450-3460.

Bertwistle, D. and Sherr, C. J. (2007). Regulation of the Arf tumor suppressor in Eμ-Myc transgenic mice: longitudinal study of Myc-induced lymphomagenesis. *Blood* **109**, 792-794.

Bertwistle, D., Zindy, F., Sherr, C. J. and Roussel, M. F. (2004). Monoclonal antibodies to the mouse p19Arf tumor suppressor protein. *Hybrid Hybridomics* **23**, 293-300.

Bierie, B. and Moses, H. L. (2006). TGFβ: the molecular Jekyll and Hyde of cancer. *Nat. Rev. Cancer* **6**, 506-520.

Bouchard, C., Lee, S., Paulus-Hock, V., Loddenkemper, C., Eilers, M. and Schmitt, C. A. (2007). FoxO transcription factors suppress Myc-driven lymphomagenesis via direct activation of *Arf*. *Genes Dev.* **21**, 2775-2787.

Bruggeman, S. W. M., Valk-Lingbeek, M. E., van der Stoop, P. P. M., Jacobs, J. J. L., Kieboom, K., Tanger, E., Hulsman, D., Leung, C., Arsenijevic, Y., Marino, S. et al. (2005). Ink4a and Arf differentially affect cell proliferation and neural stem cell self-renewal in Bmi1-deficient mice. *Genes Dev.* **19**, 1438-1443.

Colombo, E., Bonetti, P., Denchi, E. L., Martinelli, P., Zamponi, R., Marine, J. C., Helin, K., Falini, B. and Pelicci, P. G. (2005). Nucleophosmin is required for DNA integrity and p19Arf protein stability. *Mol. Cell. Biol.* **25**, 8874-8886.

Cordenonsi, M., Dupont, S., Maretto, S., Insinga, A., Imbriano, C. and Piccolo, S. (2003). Links between tumor suppressors: p53 is required for TGF-beta gene responses by cooperating with Smads. *Cell* **113**, 301-314.

Cui, W., Fowlis, D. J., Bryson, S., Duffie, E., Ireland, H., Balmain, A. and Akhurst, R. J. (1996). Tgfb1 inhibits the formation of benign skin tumors, but enhances progression to invasive spindle carcinomas in transgenic mice. *Cell* **86**, 531-542.

De Larco, J. E. and Todaro, G. J. (1978). Growth factors from murine sarcoma virus-transduced cells. *Proc. Natl. Acad. Sci. USA* **75**, 4001-4005.

de Stanchina, E., McCurrach, M. E., Zindy, F., Shieh, S. Y., Ferbeyre, G., Samuelson, A. V., Prives, C., Roussel, M. F., Sherr, C. J. and Lowe, S. W. (1998). E1A signaling to p53 involves the $p19^{ARF}$ tumor suppressor. *Genes Dev.* **12**, 2434-2442.

DeGregori, J., Leone, G., Miron, A., Jakoi, L. and Nevins, J. R. (1997). Distinct roles for E2F proteins in cell growth control and apoptosis. *Proc. Natl. Acad. Sci. USA* **94**, 7245-7250.

Derynck, R. and Zhang, Y. E. (2003). Smad-dependent and Smad-independent pathways in TGF-beta family signalling. *Nature* **425**, 577-584.

Gil, J. and Peters, G. (2006). Regulation of the INK4b-ARF-INK4a tumour suppressor locus: all for one or one for all. *Nat. Rev. Mol. Cell Biol.* **7**, 667-677.

Goldberg, M. F. (1997). Persistent fetal vasculature (PFV): an integrated interpretation of signs and symptoms associated with persistent hyperplastic primary vitreous (PHPV) LIV Edward Jackson Memorial Lecture. *Am. J. Ophthalmol.* **124**, 587-626.

Gonzalez, S., Klatt, P., Delgado, S., Conde, E., Lopez-Rios, F., Sanchez-Cespedes, M., Mendez, J., Antequera, F. and Serrano, M. (2006).

Oncogenic activity of Cdc6 through repression of the INKK4/ARF locus. *Nature* **440**, 702-706.
Goto, K., Kamiya, Y., Imamura, T., Miyazono, K. and Miyazawa, K. (2007). Selective inhibitor effects of Smad6 on Bone Morphogenetic Protein Type I receptors. *J. Biol. Chem.* **282**, 20603-20611.
Haddad, R., Font, R. L. and Reeser, F. (1978). Persistent hyperplastic primary vitreous: a clinicopathologic study of 62 cases and review of the literature. *Surv. Ophthalmol.* **23**, 123-134.
Inoue, K., Roussel, M. F. and Sherr, C. J. (1999). Induction of ARF tumor suppressor gene expression and cell cycle arrest by transcription factor DMP1. *Proc. Natl. Acad. Sci. USA* **96**, 3993-3998.
Ittner, L. M., Wurdak, H., Schwerdtfeger, K., Kunz, T., Ille, F., Leveen, P., Hjalt, T. A., Suter, U., Karlsson, S., Hafezi, F. et al. (2005). Compound developmental eye disorders following inactivation of TGFβ signaling in neural-crest stem cells. *J. Biol.* **4**, 11.0-11.16.
Jacobs, J. J. L., Kieboom, K., Marino, S., DePinho, R. A. and van Lohuizen, M. (1999). The oncogene and polycomb-group gene bmi-1 regulates cell proliferation and senescence through the ink4a locus. *Nature* **397**, 164-168.
Jacobs, J. J. L., Keblusek, P., Robanus-Maandag, E., Kristel, P., Lingbeek, M., Nederlof, P. M., van Welsem, T., van de Vijver, M. J., Koh, E. Y., Daley, G. Q. et al. (2000). Senescence bypass screen identifies TBX2, which represses Cdkn2a (p19Arf) and is amplified in a subset of human breast cancers. *Nat. Genet.* **26**, 291-299.
Kamijo, T., Zindy, F., Roussel, M. F., Quelle, D. E., Downing, J. R., Ashmun, R. A., Grosveld, G. and Sherr, C. J. (1997). Tumor suppression at the mouse INK4a locus mediated by the alternative reading frame product $p19^{ARF}$. *Cell* **91**, 649-659.
Kamijo, T., Weber, J. D., Zambetti, G., Zindy, F., Roussel, M. F. and Sherr, C. J. (1998). Functional and physical interactions of the ARF tumor suppressor with p53 and Mdm2. *Proc. Natl. Acad. Sci. USA* **95**, 8292-8297.
Kelly-Spratt, K. S., Gurley, K. E., Yasui, Y. and Kemp, C. J. (2004). p19Arf suppresses growth, progression, and metastasis of hras-driven carcinomas through p53-dependent and -independent pathways. *PLoS Biol.* **2,** E242.
Kim, W. Y. and Sharpless, N. E. (2006). The regulation of INK4/ARF in cancer and aging. *Cell* **127**, 265-275.
Kirkbride, K. C., Townsend, T. A., Bruinsma, M. W., Barnett, J. V. and Blobe, G. C. (2008). Bone morphogenetic proteins signal through the transforming growth factor-β type III receptor. *J. Biol. Chem.* **283**, 7628-7637.
Maeda, T., Hobbs, R. M., Merghoub, T., Guernah, I., Zelent, A., Cordon-Cardo, C., Teruya-Feldstein, J. and Pandolfi, P. P. (2005). Role of the proto-oncogene Pokemon in cellular transformation and ARF repression. *Nature* **433**, 278-285.
Maestro, R., Dei Tos, A. P., Hamamori, Y., Krasnokutsky, S., Sartorelli, V., Kedes, L., Doglioni, C., Beach, D. H. and Hannon, G. J. (1999). *twist* is a potential oncogene that inhibits apoptosis. *Genes Dev.* **13**, 2207-2217.
Marquardt, H., Hunkapiller, M. W., Hood, L. E., Twardzik, D. R., De Larco, J. E., Stephenson, J. R. and Todaro, G. J. (1983). Transforming growth factors produced by retrovirus-transformed rodent fibroblasts and human melanoma cells: amino acid sequence homology with epidermal growth factor. *Proc. Natl. Acad. Sci. USA* **80**, 4684-4688.
Marquardt, H., Hunkapiller, M. W., Hood, L. E. and Todaro, G. J. (1984). Rat transforming growth factor Type **1**, structure and relation to epidermal growth factor. *Science* **223**, 1079-1082.
Martin, A. C., Thornton, J. D., Liu, J., Wang, X. F., Zuo, J., Jablonski, M. M., Chaum, E., Zindy, F. and Skapek, S. X. (2004). Pathogenesis of persistent hyperplastic primary vitreous in mice lacking the Arf tumor suppressor gene. *Invest. Ophthalmol. Vis. Sci.* **45**, 3387-3396.
Massague, J., Blain, S. W. and Lo, R. S. (2000). TGFβ signaling in growth control, cancer, and heritable disorders. *Cell* **103**, 295-309.
McKeller, R. N., Fowler, J. L., Cunningham, J. J., Warner, N., Smeyne, R. J., Zindy, F. and Skapek, S. X. (2002). The Arf tumor suppressor gene promotes hyaloid vascular regression during mouse eye development. *Proc. Natl. Acad. Sci. USA* **99**, 3848-3853.
Molofsky, A. V., He, S., Bydon, M., Morrison, S. J. and Pardal, R. (2005). Bmi-1 promotes neural stem cell self-renewal and neural development but not mouse growth and survival by repressing the p16Ink4a and p19Arf senescence pathways. *Genes Dev.* **19**, 1432-1437.
Nomura, M. and Li, E. (1998). Smad2 role in mesoderm formation, left-right patterning and craniofacial development. *Nature* **393**, 786-790.
Palmero, I., Pantoja, C. and Serrano, M. (1999). $p19^{ARF}$ links the tumor suppressor p53 to Ras. *Nature* **395**, 127.
Ross, S. and Hill, C. S. (2008). How the Smads regulate transcription. *Int. J. Biochem. Cell Biol.* **40**, 383-408.
Saika, S., Saika, S., Liu, C. Y., Azhar, M., Sanford, L. P., Doetschman, T., Gendron, R. L., Kao, C. W. and Kao, W. W. (2001). TGFbeta2 in corneal morphogenesis during mouse embryonic development. *Dev. Biol.* **240**, 419-432.
Sanford, L. P., Ormsby, I., Gittengerger-de Groot, A. C., Sariola, H., Friedman, R., Boivin, G. P., Cardell, E. L. and Doetschman, T. (1997). TGFb2 knockout mice have multiple developmental defects that are non-overlapping with other TGFb knockout phenotypes. *Development* **124**, 2659-2670.
Seay, U., Sedding, D., Krick, S., Hecker, M., Seeger, W. and Eickelberg, O. (2005). Transforming growth factor-b-dependent growth inhibition in primary vascular smooth muscle cells is p38-dependent. *J. Pharmacol. Exp. Ther.* **315**, 1005-1012.
Sharpless, N. E., Ramsey, M. R., Balasubramanian, P., Castrillon, D. H. and DePinho, R. A. (2004). The differential impact of p16(INK4a) or p19(ARF) deficiency on cell growth and tumorigenesis. *Oncogene* **23**, 379-385.
Sherr, C. J. (2006). Divorcing ARF and p53: an unsettled case. *Nat. Rev. Cancer* **6**, 663-673.
Sherr, C. J. and DePinho, R. A. (2000). Cellular senescence: mitotic clock or culture shock? *Cell* **102**, 407-410.
Silva, R. L., Thornton, J. D., Martin, A. C., Rehg, J. E., Bertwistle, D., Zindy, F. and Skapek, S. X. (2005). Arf-dependent regulation of Pdgf signaling in perivascular cells in the developing mouse eye. *EMBO J.* **24**, 2803-2814.
Smith, A. P., Verrecchia, A., Faga, G., Doni, M., Perna, D., Martinato, F., Guccione, E. and Amati, B. (2009). A positive role for Myc in TGFβ-induced Snail transcription and epithelial-to-mesenchymal transition. *Oncogene* **28**, 422-430.
Thornton, J. D., Swanson, D. J., Mary, M. N., Pei, D., Martin, A. C., Pounds, S., Goldowitz, D. and Skapek, S. X. (2007). Persistent hyperplastic primary vitreous due to somatic mosaic delection of the Arf tumor suppressor. *Invest. Ophthalmol. Vis. Sci.* **48**, 491-499.
Warot, X., Fromental-Ramain, C., Fraulob, B., Chambon, P. and Dolle, P. (1997). Gene dosage-dependent effects of the Hoxa-13 and Hoxd-13 mutations on morphogenesis of the terminal parts of the digestive and urogenital tracts. *Development* **124**, 4781-4791.
Weinstein, M., Yang, S., Li, C., Xu, X., Gotay, J. and Deng, C. X. (1998). Failure of egg cylinder elongation and mesoderm induction in mouse embryos lacking the tumor suppressor smad2. *Proc. Natl. Acad. Sci. USA* **95**, 9378-9383.
Zhao, S. and Overbeek, P. A. (2001). Elevated TGFb signaling inhibits ocular vascular development. *Dev. Biol.* **237**, 45-53.
Zhu, Y., Richardson, J. A., Parada, L. F. and Graff, J. M. (1998). Smad3 mutant mice develop metastatic colorectal cancer. *Cell* **94**, 703-714.
Zindy, F., Quelle, D. E., Roussel, M. F. and Sherr, C. J. (1997). Expression of the p16INK4a tumor suppressor versus other INK4 family members during mouse development and aging. *Oncogene* **15**, 203-211.
Zindy, F., Eischen, C. M., Randle, D. H., Kamijo, T., Cleveland, J. L., Sherr, C. J. and Roussel, M. F. (1998). Myc signaling via the ARF tumor suppressor regulates p53-dependent apoptosis and immortalization. *Genes Dev.* **12**, 2424-2433.
Zindy, F., Williams, R. T., Baudino, T. A., Rehg, J. E., Skapek, S. X., Cleveland, J. L., Roussel, M. F. and Sherr, C. J. (2003). Arf tumor suppressor promoter monitors latent oncogenic signals *in vivo*. *Proc. Natl. Acad. Sci. USA* **100**, 15930-15935.